Histomorphometric Evaluation of Bioceramic Molecular Impregnated and Dual Acid-Etched Implant Surfaces in the Human Posterior Maxilla

Jamil Awad Shibli, DDS, MS, PhD;* Sauro Grassi, DDS, MS;† Adriano Piattelli, MD, DDS;‡ Gabriele E. Pecora, MD, DDS;§ Daniel S. Ferrari, DDS, MS;† Tatiana Onuma, DDS;† Susana d'Avila, DDS, MS, PhD;¶ Paulo G. Coelho, DDS, PhD;** Raquel Barros, DDS, MS;†† Giovanna Iezzi, DDS, PhD‡‡

ABSTRACT

Background: Physical and bioceramic incorporation surface treatments at the nanometer scale showed higher means of bone-to-implant contact (BIC) and torque values compared with surface topography at the micrometer scale; however, the literature concerning the effect of nanometer scale parameters is sparse.

Purpose: The aim of this study was to evaluate the influence of two different implant surfaces on the percentage bone-to-implant contact (BIC%) and bone osteocyte density in the human posterior maxilla after 2 months of unloaded healing.

Materials and Methods: The implants utilized presented dual acid-etched (DAE) surface and a bioceramic molecular impregnated treatment (Ossean®, Intra-Lock International, Boca Raton, FL, USA) serving as control and test, respectively. Ten subjects (59 ± 9 years of age) received two implants (one of each surface) during conventional implant surgery in the posterior maxilla. After the non-loaded period of 2 months, the implants and the surrounding tissue were removed by means of a trephine and were non-decalcified processed for ground sectioning and analysis of BIC%, bone density in threaded area (BA%), and osteocyte index (Oi).

Results: Two DAE implants were found to be clinically unstable at time of retrieval. Histometric evaluation showed significantly higher BIC% and Oi for the test compared to the control surface ($p < .05$), and that BA% was not significantly different between groups. Wilcoxon matched pairs test was used to compare the differences of histomorphometric variables between implant surfaces. The significance test was conducted at a 5% level of significance.

Conclusion: The histological data suggest that the bioceramic molecular impregnated surface-treated implants positively modulated bone healing at early implantation times compared to the DAE surface.

KEY WORDS: dental implants, human histology, implant surface topography/nanostructure, posterior maxilla, surface

Long-term investigations have documented the high predictability of implant-supported restorations in edentulous patients.[1,2] However, studies have demonstrated that the survival of dental implants placed in posterior maxilla was inferior to those placed in the anterior mandible, where the bone density is frequently higher.[3,4] The demand for improved dental implant survival at sites of lower bone density, such as the posterior

*Assistant professor, Department of Periodontology, Dental Research Division and Head of Oral Implantology Clinic, Guarulhos University, Guarulhos, SP, Brazil; †graduate student, Department of Periodontology, Dental Dental Research Division, Guarulhos University, Guarulhos, SP, Brazil; ‡professor, Department of Oral Medicine and Oral Pathology, Dental School, University of Chieti-Pescara, Chieti, Italy; §private practice, Rome, Italy; ¶professor, Oral Implantology Clinic, Guarulhos University, Guarulhos, SP, Brazil; **adjunct professor, Department of Biomaterials and Biomimetics, New York University, New York, USA; ††graduate student, Department of Bucco-Maxillo-Facial Surgery and Traumatology and Periodontology, School of Dentistry of Ribeirão Preto, University of São Paulo, Ribeirão Preto, SP, Brazil; ‡‡research fellow, Department of Oral Medicine and Oral Pathology, Dental School, University of Chieti-Pescara, Chieti, Italy

The authors report no conflicts of interest related to this study.

Reprint requests: Prof. Jamil Awad Shibli, Centro de Pós-Graduação, Pesquisa e Extensão-CEPPE, Universidade Guarulhos, R. Dr. Nilo Peçanha, 81 – 6°. Andar – Prédio U, 07011-040 Guarulhos, SP, Brazil; e-mail: jashibli@yahoo.com

DOI 10.1111/j.1708-8208.2009.00174.x

maxilla, has prompted researchers to look for implant design alterations that would increase the early host-to-implant response and the system temporal biomechanics. Among design modifications, surface alteration has been by far the most investigated subject.

Because the implant surface is the first part of the biomedical device to interact with the host, body fluids and cell interaction to micrometer scale features such as grooves, ridges, and wells, as well as different chemistries have been investigated.[5–7] Previous studies[8–12] developed by our group have demonstrated that rough implant surface topography at micrometer scale presented improved osteogenic response compared to machined dental implant surfaces under unloaded conditions.

While establishment of osseointegration and rapid biomechanical fixation has been demonstrated for moderately rough surfaces (average roughness, Ra, ranging from 0.5 to 2 μm)[13] compared to as-turned/machined surfaces, recent studies have demonstrated that physicochemical features on the nanometer scale may further enhance the host-to-implant response at early times after implantation.[13–17]

Surface properties in the nanometer scale may further modulate the characteristics of the protein layer adhesion in our body; the nanoscale structure of the extracellular matrix provides an essential and natural web of nanofibers to support cells and depict an instructive background to guide their behavior. The fibers of the extracellular matrix, basement membrane, their interconnecting nanopores, and hydroxyapatite crystals found in natural bone present nanoscaled dimensions.[18] Thus, the application of nanotechnology for the alteration of texture and chemistry in dental implant topography may result in varied cell behavior, ranging from alterations in adhesion, orientation, mobility, and surface antigen display of the pre-osteogenic and osteogenic cells. Complementary, nanoscale features may also affect the adsorption and conformation of integrin-binding proteins, changing the availability of binding sites and modify integrin signaling.[19,20]

Physical and bioceramic incorporation surface treatments at nanometer scale have shown higher means of bone-to-implant contact (BIC) and torque values compared with rough implant surface topography at micrometer scale.[13,15] While controlled animal studies report surface physicochemical modification in the nanometer scale, the literature concerning the effect of nanometer scale parameters is sparse.

Thus, the aim of this controlled clinical study was to evaluate the early host-to-implant parameters (BIC%, bone density in threaded area [BA%], and osteocyte index [Oi]) to different implant surface treatments in the human posterior maxilla after an unloaded healing period of 2 months.

MATERIALS AND METHODS

Subjects

Ten totally edentulous subjects (six women; four men), with a mean age of 53 ± 9 years, referred to the Department of Periodontology (Dental Research Division, Guarulhos University, Brazil) for implant therapy, were included in this study. Exclusion criteria included pregnancy, nursing, smokers, and any systemic condition that could affect bone healing. The Ethics Committee for Human Clinical Trials at Guarulhos University approved the study protocol.

Experimental Implant Surface Topographies

In this study, screw-shaped implants were prepared with two surface morphologies: bioceramic molecular impregnation (Ossean®, Intra-Lock International, Boca Raton, FL, USA) and dual acid-etched (DAE) (Intra-Lock International) surface topographies (Figure 1). Previous physicochemical characterization has determined that the Ossean implant surface presented increased texture in the micrometer[13] (qualitatively determined through scanning electron microscopy, see Figure 1) and in the nanometer scale compared to the DAE surface.[13] The nanoscale topographies evaluated by atomic force microscopy over an area of 20 × 20 μm depicted higher arithmetic average of the absolute values (Ra, 157.1 ± 38.2 nm vs 114.6 ± 31.3 nm) and root mean square (266.2 ± 49 nm vs 188.0 ± 36.2 nm) values BGB/AA compared to DAE surface, respectively.[13] In addition, Auger and x-ray photoelectron spectroscopy depicted calcium phosphate (CaP) at submicrometer texturing. No particle was visible at the maximum SEM resolution (200,000×).[13]

Implant Surgery

Twenty implants were used in this study ($n = 10$ DAE and $n = 10$ BGB/AA experimental implants). The implants were placed under aseptic conditions as previously described.[8,9] After crestal incision, mucoperiosteal flaps were raised and conventional implants were

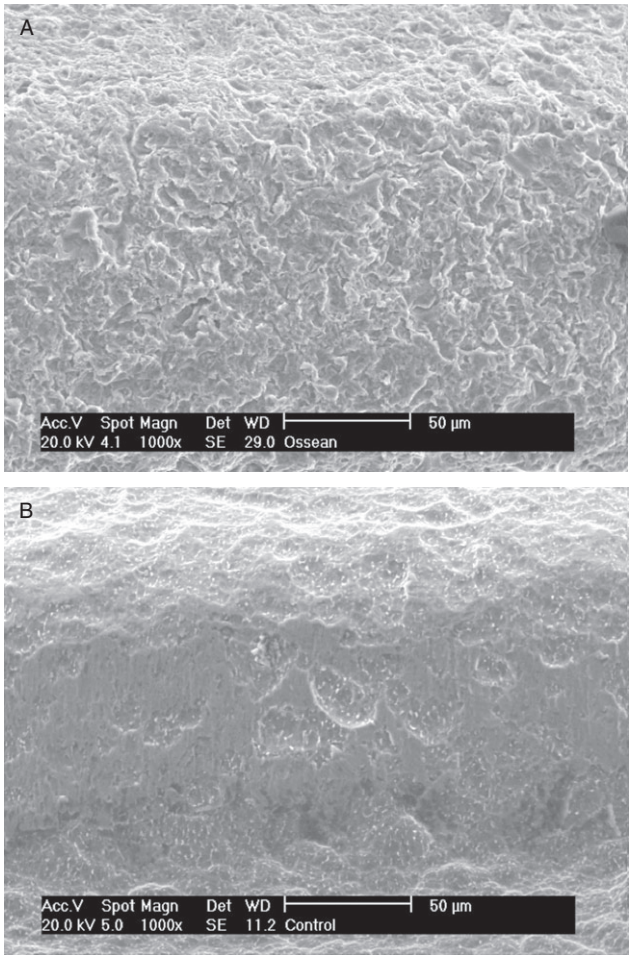

Figure 1 Scanning electron microphotograph of the implant surface topographies evaluated *A*, Ossean® and *B*, dual acid-etched surface.

placed in the totally edentulous maxilla in accordance with the surgical/prosthetic plan prepared for each patient. Next, the experimental implant groups were randomly placed in the molar region, that is, posterior to the most distal conventional implant. The implant recipient sites were prepared with a 2.8 mm-diameter twist drill in soft bone. All drilling and implant placement procedures were completed under profuse irrigation with sterile saline solution. If during placement an implant showed low primary stability, a backup surgical site was prepared. The flaps were sutured to cover the micro-implants.

Postoperative medication included clindamycin administered three times a day (1,200 mg/day) for 7 days a week. The sutures were removed after 10 days. To enable subjects to control postoperative dental biofilm, 0.12% chlorhexidine rinses were prescribed, twice a day for 14 days.

After a healing period of 2 months, during the two-stage surgery of the conventional implants, the experimental implants and surrounding tissues were retrieved with a 4.0-millimeter-wide trephine bur, and the specimens were initially fixed by immersion in neutral formalin at 4%.

Specimen Processing and Histomorphometric Analyses

Following retrieval and initial fixation, the implants and surrounding tissues were stored in 10% buffered formalin and processed to obtain thin ground sections (Precise 1 Automated System, Assing, Rome, Italy) as previously described.[21] The specimens were dehydrated in an ascending series of alcohol rinses, and embedded in a glycolmethacrylate resin (Technovit® 7200, VLC, Kulzer, Wehrheim, Germany). After polymerization, the specimens were sectioned longitudinally along the implant long axis with a high-precision diamond disk at about 150 µm and ground down to ~30 µm. Two to three slides were obtained per implant. The slides were stained with acid fuchsin and toluidine blue. Percentage of BIC (BIC%) was defined as the amount of mineralized bone in direct contact with the implant surface. The measurements were made throughout the entire extent of the implant. The BA% was defined as the fraction of mineralized bone tissue within the threaded area. All threads were measured and included in the statistical analysis.

The Oi was calculated using the equation Oi = N.Ot/B.Ar, where N.Ot is the number of osteocytes observed at 200× magnification on the section plane for an infinitely thin section, and B.Ar is the total area of the evaluated bone expressed in μm^2 (or in square pixels). The Oi was assessed near and at a distance from the implant surface. Oi in a 50 µm-wide zone lateral to the implant surface was measured bilaterally (adjacent area). The specimens were analyzed under a transmitted light microscope that was connected to a high-resolution video camera (3CCD, JVC KY-F55B, JVCs, Yokohama, Japan) and interfaced to a monitor and computer. This optical system was associated with a digitizing pad (Matrix Vision GmbH, Oppenweiler, Germany) and controlled by a software package with image-capturing capabilities (Image-Pro® Plus 4.5, Media Cybernetics, Inc., Immagini & Computer Snc, Milano, Italy). Bone area and cell number were analyzed using image managing software (Adobe Photoshop CS, version 8.0.1, Adobe Systems, Beaverton, OR, USA) and

image analysis software (Image J1.32j, Wayne Rasband, National Institutes of Health, Bethesda, MD, USA). All images were calibrated using the Pythagorean theorem for distance calibration, which reported the number of pixels between two selected points.

The mean and standard deviation of histomorphometric variables were calculated for each implant, then for each group. Wilcoxon matched pairs test was used to compare the differences of histomorphometric variables between implant surfaces. The significance test was conducted at a 5% level of significance.

RESULTS

Clinical Observations

Two implants with DAE treatment showed no osseointegration and were not included in the evaluation. The remaining 18 experimental implants were clinically stable at the time of retrieval and did not present clinical evidence of inflammation or infection.

Histological and Histomorphometric Results

Overall, the bone surrounding the implants was healthy. Mineralized tissue was present at the interface with both implant surfaces. A newly formed bone was observed in close contact with the implant surface, especially in the coronal area. The woven structure of the newly formed bone was separated from the pristine bone by cement lines. In some portions of the bone-implant interface, in the coronal and middle portions of the implants, osteoblasts were depositing osteoid matrix directly onto the dental implant surface, mainly on the Ossean implant surface (Figures 2 and 3). In addition, a thin layer of bone trabeculae was interposed between the old bone and the Ossean implant surface, and a thin layer of dense connective tissue was observed in this area. A large portion of the Ossean implant appeared to be lined by bone trabeculae.

In contrast, smaller amounts of new bone apposition were observed along the DAE implant surface, especially inside the implant threads (Figure 4). Detailed observation of the bone in proximity to the DAE surface revealed bone tissue with immature appearance compared to bone in proximity with the Ossean (see Figure 4, C). In general, the newly formed bone surrounding both surfaces showed early stages of maturing and remodeling. Neither epithelial downgrowth nor inflammatory cell infiltrate was observed in both evaluated implants.

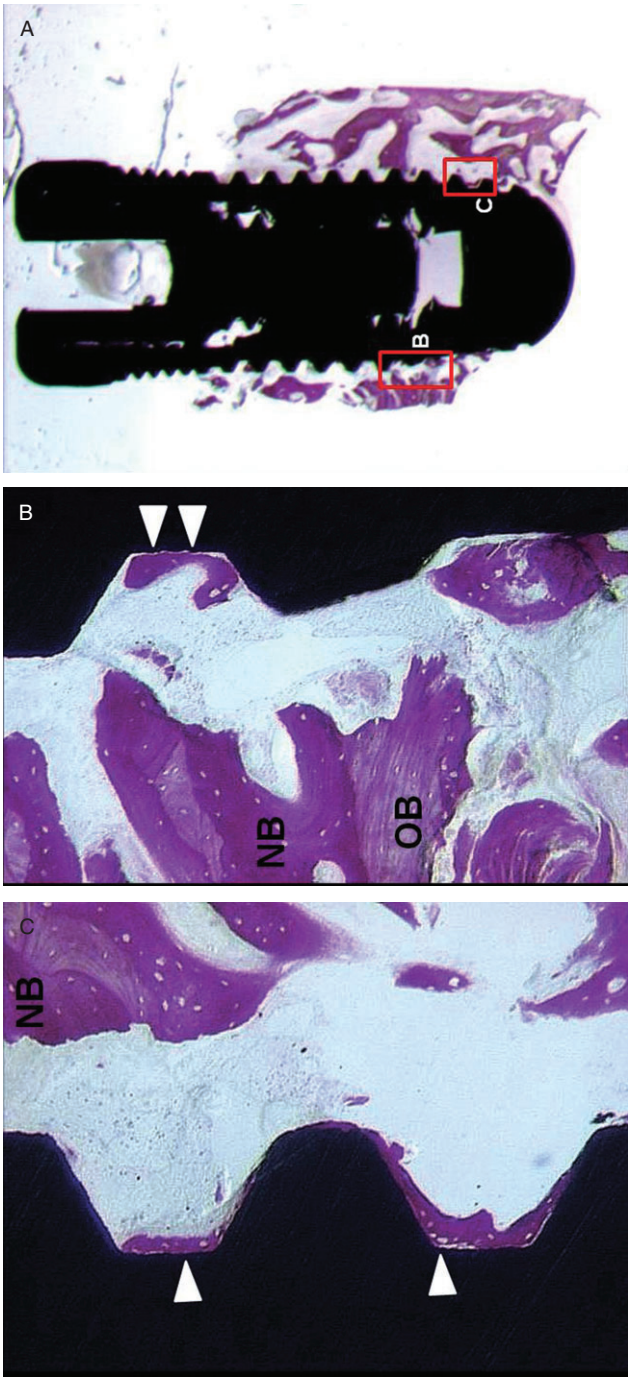

Figure 2 Histologic ground section of Ossean® implant. *A*, The old bone (OB) was mostly lamellar. *B* and *C*, Larger magnification of the lateral frame areas in the section shown in *A*. Apposition of new bone (NB) is depicted in close contact (arrowhead) with the implant surface. Reversal lines showing the limits between OB and new bone (NB) (basic fuchsin and toluidine blue staining, original magnification ×200).

BIC% was statistically higher for Ossean implant surfaces (Table 1). BIC% values for the DAE surface ranged between 10 and 29.65%, while the mean values for the Ossean surface treatment ranged between 15.98

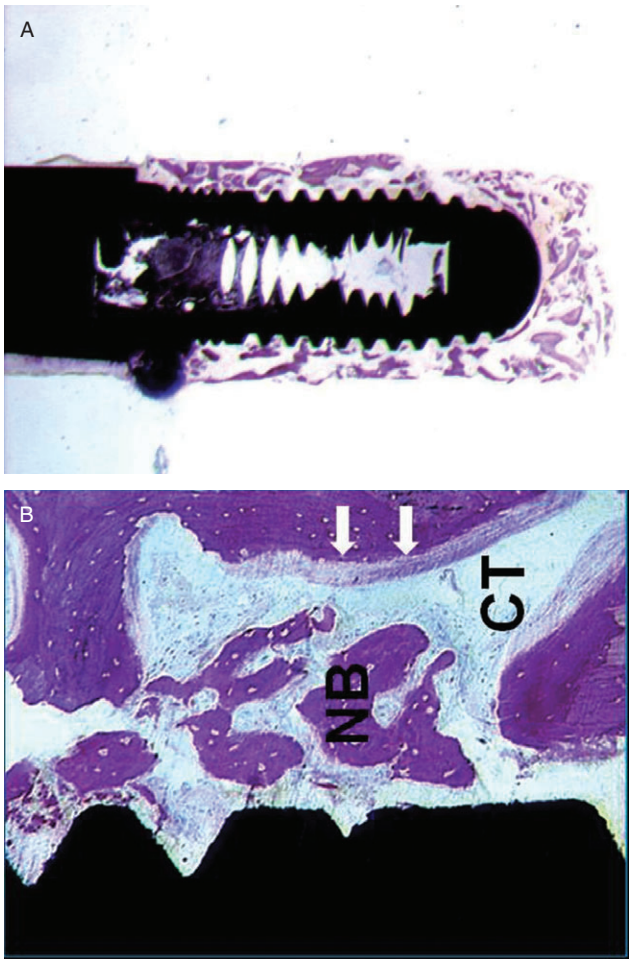

Figure 3 Histologic ground section of the Ossean® implant surface. *A*, The Ossean surface depicted newly formed bone with connecting bridges between the new bone trabeculae and the implant surface (basic fuchsin and toluidine blue staining, original magnification ×12). *B*, Ground section of the Ossean implant surface presenting newly formed bone exhibited early stages of maturation and remodelation. The newly formed bone (NB) is close to implant surface (arrows), suggesting contact osteogenesis (basic fuchsin and toluidine blue staining, original magnification ×100).

and 80.5%. Ossean implants presented also higher mean bone density values (BA%) in the thread area, however, not significant ($p > .05$).

The Oi at distance and near to implant surface was significantly higher for Ossean implants ($p < .05$) (Table 2). Oi adjacent and at distance to Ossean implant surfaces averaged 37.88/mm and 31.48/mm^2, respectively, whereas DAE surface depicted lower means for both Oi indexes at 19.23 and 19.79/mm^2. In addition, the bioceramic molecular impregnated surface depicted higher means for both Oi index at woven and lamellar bone ($p < .05$).

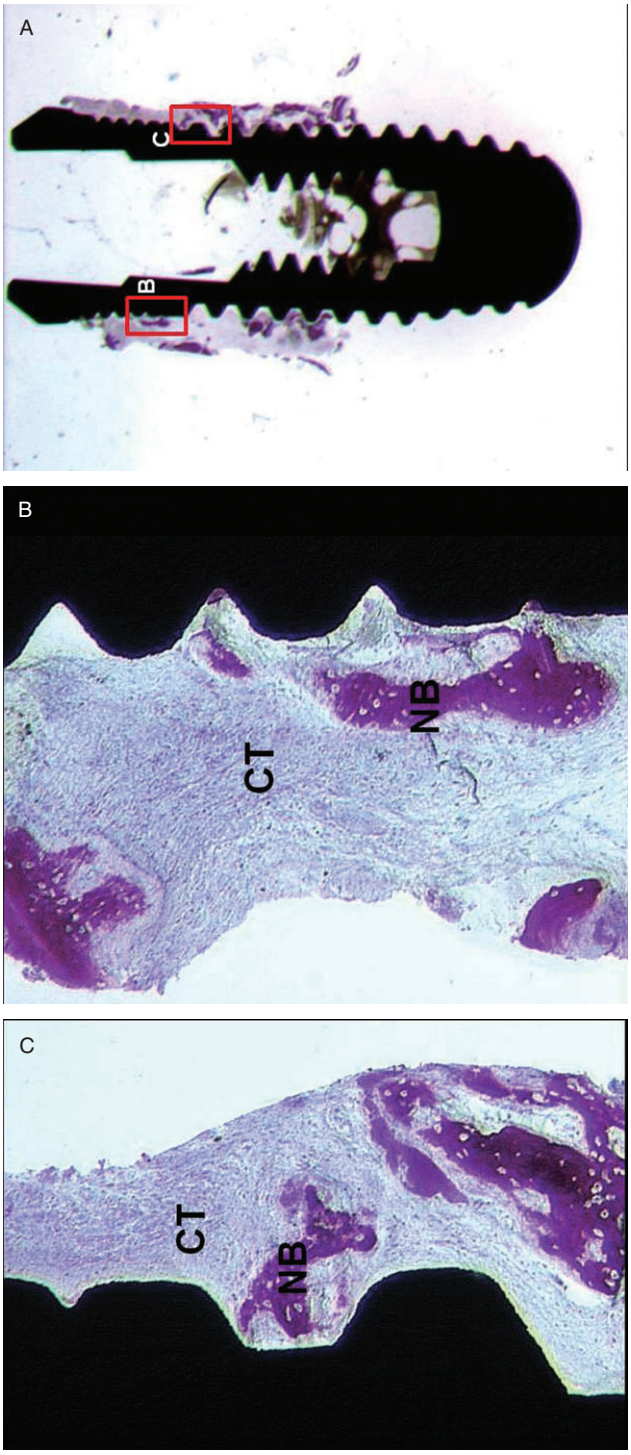

Figure 4 *A*, Histological ground section of the dual acid-etched surface after 2 months of healing depicting the newly formed bone showing early maturing and remodeling stages. Note the lack of connecting bridges between the new bone trabeculae and the implant surface (basic fuchsin and toluidine blue staining, original ×12 magnification). *B* and *C*, A larger magnification of the lateral frame areas in the section shown in *A*. The newer bone (NB) tissue shows no contact with the implant surface with presence of connective tissue (CT) (basic fuchsin and toluidine blue staining, original ×200 magnification).

TABLE 1 Mean and Standard Deviation of Bone-to-Implant Contact Percentages (BIC%), Bone Density in the Threaded Area (BA%), to Implants with (Ossean) and Dual Acid-Etched (DAE) Surfaces in Posterior Maxilla (n = 10 subjects). Wilcoxon test ($p < .05$)

	Bioceramic Grit-Blated/ Acid Etched (Ossean)		Dual Acid-etched (DAE)			
Histometric Variables	Mean ± SD	Range	Mean ± SD	Range	p Value	CI 95%
BIC%	43.38 ± 22.52	15.98–80.5	21.82 ± 7.03	10.0–29.65	0.004	15.31–62.19
BA%	33.96 ± 14.38	12.45–57.09	25.70 ± 12.39	11.12–45.65	0.578	14.24–47.26

DISCUSSION

This study demonstrated increased BIC% and Oi index values to bioceramic molecular impregnation compared to DAE surfaces. Recently, several studies have shown that CaP-based material at nanometer scale influence early bone healing at the tissue/implant interface increasing bone formation.[13–16] The Ossean implant was prepared based on molecular integration of $CaPO_4$ on the titanium oxide surface. It has been demonstrated that CaP-coated surfaces increase the levels of platelet activation providing an initial stimulus to accelerate early bone healing. The addition of Ca and P to implant surface increases not only the complexity of implant surface topography, but also the platelet activation.[22] However, these processes did not influence the bone density in the threads area (see Table 2). The authors speculated that Ossean surface topography influenced the bone tissue response at the interface and not at bone density, at least after 2 months of unloaded healing.

A thin newly formed bone covered a large portion of the Ossean implant threads. This feature showed that osteoblasts were activated by direct contact with the Ossean surface, suggesting contact osteogenesis.[6,23] However, woven bone was also found on both surface topographies at a certain distance from the pristine bone, or distance osteogenesis.[6,23] Complementary, some histological, sections showed osteoblasts lining the newly formed bone, although this feature was less evident in the DAE surfaces.

The Ossean surface topography presented higher amount of BIC%, indicating that the cellular reaction differed between the implant surfaces.[24,25] Previous studies[13,26] have shown, in a dog model, that Ossean surface inserted in the cortical bone did not increase the BIC%, but increased implant biomechanical fixation at early times in vivo compared to the same DAE surface utilized as control in the present study, indicating that the overall system biomechanics was improved by the surface treatment. This occurrence may be explained based on bone quality and quantity. The cortical bone offers more organized vital structure when compared with the type IV bone present in the posterior maxilla. Our results depicted higher BIC% in areas of low bone density, suggesting that the CaP-based surface modification played a pivotal role in early host-to-implant interaction in bone presenting low density levels.

Osteogenesis at the bone-implant interface is influenced by several mechanisms. A series of coordinated

TABLE 2 Mean and Standard Deviation of Osteocyte Density (Oi) at Distance, Next to, in the Woven, and Lamellar Bone, to Implants with (Ossean®) and Dual Acid-Etched (DAE) Surfaces in Posterior Maxilla (n = 10 subjects)

	Bioceramic Grit-Blated/ Acid Etched (Ossean)		Dual Acid Etched (DAE)			
Osteocyte Index (mm^2)	Mean ± SD	Range	Mean ± SD	Range	p Value	CI 95%
Next to distance	37.88 + 5.35	29.65–45.21	19.23 + 3.08	15.50–25.21	0.031	16.38–43.50
	31.48 + 7.04	21.65–38.32	19.79 + 4.56	12.23–23.32	0.125	10.56–42.69
Woven	39.38 + 3.76	34.50–45.21	16.80 + 3.50	11.50–19.65	0.032	13.53–43.34
Lamellar	35.33 + 6.43	24.5–41.60	16.37 + 3.40	11.50–19.65	0.028	13.17–42.30

Wilcoxon test ($p < .05$).

events, including protein adsorption, proliferation, and bone tissue deposition might be affected by the different surface topographies. At the nanoscale level and beyond, the bone tissue contains complex characteristics of topographic pits, protusions, and fibers, arising in bone tissue from the nanocrystalline-mineralized osteoid. In turn, each of these events is affected by physicochemical interaction between the molecules and cells in the peri-implant area.[25] The implant surface chemical and topographical properties, as well as the specific properties of individual proteins, determine the organization of the adsorbed protein layer.

Research on implant surface topography and chemistry have shown that implant surface topography itself can affect not only the osteoblast gene expression, but also cell differentiation into osteoblasts.[27,28] The authors also suggested that cell interaction with extracellular matrix components, and actin cytoskeleton organization associated with implant surface topography can influence cell gene expression.[27,28]

Complementary, the results of the present study have shown a higher and statistically significant osteocyte density for Ossean surfaces at bone regions in close proximity with the implant, but not at regions farther away from the surace, suggesting a higher osteoblast incorporation rate as a function of time compared to DAE and thus more rapid bone growth around Ossean surfaces.

The role of the osteocytes remains partially unresolved, but an important role in the regulation of skeleton remodeling has been suggested.[29] Alterations in the osteocyte environment produce a release of growth factors and cytokines that affect osteoblasts and osteoclasts. Thus, the Ossean surface topography/chemistry may play an important role in the process because osteocyte incorporation takes place to higher degrees over a given period of time.

Woven bone has been found to have a four to eight times higher number of osteocytes than lamellar bone.[30] The Ossean surface positively influenced the density of osteocytes in peri-implant bone, including woven bone. Osteocyte density has been reported to be inversely proportional to bony mass,[31] and the osteocytes seem to be involved in the maintenance of the functional matrix. Consequently, it may be suggested that the nanoscale topography and/or chemistry present in the Ossean surface influenced the Oi. Thus, while significantly different values of Oi were observed between surfaces, indicating higher integration rates at regions in close proximity to the implant surface, further characterization and correlation between the Oi and other histomorphometric parameters are encouraged.

Within the limits of the present study, the histological data in humans confirmed that the surface topography and/or calcium phosphate incorporated at the molecular level on the surfaces (Ossean) positively influenced/modulated early bone tissue response under unloaded conditions.

REFERENCES

1. van Steenberghe D, Quirynen M, Naert I. Survival and success rates with oral endosseous implants. In: Lang NP, Karring T, Lindhe J, eds. Procedings of the 3rd European worshop on periodontology. Berlin, Germany: Quintessence Books, 1999:242–254.
2. Naert I, Alsaadi G, Quirynen M. Prosthetic aspects and patient satisfaction with two-implant-retained mandibular overdentures: a 10-year randomized clinical study. Int J Prosthodont 2004; 17:401–410.
3. Friberg B, Jemt T, Lekholm U. Early failures in 4641 consecutively placed Bränemark dental implants. A study from stage I surgery to the connection of completed prostheses. Int J Oral Maxillofac Implants 1991; 6:142–146.
4. Jaffin RA, Berman CL. The excessive loss of Branemark fixtures in type IV bone. A 5-year analysis. J Periodontol 1991; 62:2–4.
5. Buser D, Schenk RK, Steinemann S, Fiorellini JP, Fox CH, Stich H. Influence of surface characteristics on bone integration of titanium implants. A histomorphometric study in miniature pigs. J Biomed Mater Res 1991; 25:889–902.
6. Davies JE. Mechanisms of endosseous integration. Int J Prosthodont 1998; 11:391–401.
7. Wennerberg A, Albrektsson T, Andersson T, Andersson B, Krohl GG. A histomorphometric and removal torque study of screw-shaped titanium implants with three different surface topographies. Clin Oral Implants Res 1995; 6:24–30.
8. Shibli JA, Grassi S, de Figueiredo LC, et al. Influence of implant surface topography on early osseointegration: a histological study in human jaws. J Biomed Mater Res B Appl Biomater 2007; 80:377–385.
9. Grassi S, Piattelli A, de Figueiredo LC, et al. Histologic evaluation of early human bone response to different implant surfaces. J Periodontol 2006; 77:1736–1743.
10. Shibli JA, Grassi S, de Figueiredo LC, et al. Human peri-implant bone response to turned and oxidized titanium implants inserted and retrieved after 2 months. Implant Dent 2007; 16:252–259.
11. Grassi S, Piattelli A, Ferrari DS, et al. Histologic evaluation of human bone integration on machined and sandblasted

acid-etched titanium surfaces in type IV bone. J Oral Implantol 2007; 33:8–12.
12. Shibli JA, Feres M, de Figueiredo LC, Iezzi G, Piattelli A. Histological comparison of bone to implant contact in two types of dental implant surfaces: a single case study. J Contemp Dent Pract 2007; 8:29–36.
13. Marin C, Granato R, Suzuki M, Gil JN, Piattelli A, Coelho PG. Removal torque and histometric evaluation of bioceramic grit-blasted/acid-etched and dual acid-etched implant surfaces: an experimental study in dogs. J Periodontol 2008; 79:1942–1949.
14. Meirelles L, Arvidsson A, Andersson M, Kjellin P, Albrektsson T, Wennerberg A. Nano hydroxyapatite structures influence early bone formation. J Biomed Mater Res A 2008; 87:299–307.
15. Ogawa T, Saruwatari L, Takeuchi K, Aita H, Ohno N. Ti nano-nodular structuring for bone integration and regeneration. J Dent Res 2008; 87:751–756.
16. Meirelles L, Currie F, Jacobsson M, Albrektsson T, Wennerberg A. The effect of chemical and nanotopographical modifications on the early stages of osseointegration. Int J Oral Maxillofac Implants 2008; 23:641–647.
17. Mendes VC, Moineddin R, Davies JE. Discrete calcium phosphate nanocrystalline deposition enhances osteoconduction on titanium-based implant surface. J Biomed Mater Res Part A 2008. doi 10.1002/jbm.a.32126
18. Stevens MM, George JH. Exploring and engineering the cell surface interface. Science 2005; 310:1135–1138.
19. Webster TJ, Schadler LS, Siegel RW, Bizios R. Mechanisms of enhanced osteoblast adhesion on nanophase alumina involve vitronectin. Tissue Eng 2001; 7:291–301.
20. Biggs MJ, Richards RG, Gadegaard N, McMurray RJ, Affrossman S, Wilkinson CD, Oreffo RO, Dalby MJ. Interactions with nanoscale topography: Adhesion quantification and signal transduction in cells of osteogenic and multipotent lineage. J Biomed Mater Res A 2009; DOI: 10.1002/jbm.a.32196. [Epub ahead of print]
21. Piattelli A, Scarano A, Quaranta M. High-precision, cost-effective system for producing thin sections of oral tissues containing dental implants. Biomaterials 1997; 18:577–579.
22. Kikuchi L, Park JY, Victor C, Davies JE. Platelet interactions with calcium-phosphate-coated surfaces. Biomaterials 2005; 26:5285–5295.
23. Davies J. Bone bonding at natural and biomaterial surfaces. Biomaterials 2007; 28:5058–5067.
24. Schneirder GB, Zaharias R, Seabold D, Keller J, Stanford C. Differentiation of preosteoblasts is affected by implant surface microtopographies. J Biomed Mater Res 2004; 64A:462–468.
25. Schneider GB, Perinpanayagam H, Clegg M, et al. Implant surface roughness affect osteoblast gene expression. J Dent Res 2003; 82:372–376.
26. Coelho PG, Cardaropoli G, Suzuki M, Lemons JE. Early healing of nanothickness bioceramic coating on dental implants. An experimental study in dogs. J Biomed Mater Res B Appl Biomater 2008; DOI: 10.1002/jbm.b.31090. [Epub ahead of print]
27. Martin JY, Schwartz Z, Hummert TW, Schraub DM, Simpson J, Cochran DL. Effect of titanium surface roughness on proliferation, differentiation and protein syntesis of human osteoblast-like cells. J Biomed Mater Res 1995; 29:389–401.
28. Schwartz Z, Lohmann CH, Oefinger J, Bonewald LF, Dean DD, Boyan BD. Implant surface characteristics modulate differentiation behavior of cells in the osteoblastic lineage. Adv Dent Res 1999; 13:38–48.
29. Metz LN, Martin RB, Turner AS. Histomorphometric analysis of the effects of osteocyte density on osteonal morphology and remodelling. Bone 2003; 33:753–759.
30. Hernandez CJ, Majeska RJ, Schaffler MB. Osteocyte density in woven bone. Bone 2004; 35:1095–1099.
31. Cullinane DM. The role of osteocytes in bone regulation: mineral homeostasis versus mechanoreception. J Musculoskelet Neuronal Interact 2002; 2:242–244.